研 究 論 文

大韓熔接學會誌
第11卷第3號1993年9月
Journal of the Korean
Welding Society
Vol. 11. No. 3. Sep., 1993

용접 잔류응력 해석을 위한 Heat Input Model 개발

심 용 래* · 이 성 근**

Modeling of Welding Heat Input for Residual Stress Analysis

Yong Lae Shim* and Sung Geun Lee**

Key Words : Welding(용접), Residual Stress(잔류응력), Finite Element Method(유한요소법), Multipass Welds(다층용접), Lumped Model

요 약

용접에서 발생하는 열응력 및 잔류응력을 해석하기 위한 유한요소용 모델을 개발하였다. 여러가지 변수의 연구를 통하여 Ramp heat input function과 Lumped 모델을 제시하였다. 용접부에 열입력을 점차적으로 주기 위하여 Ramp heat input을 이용하였으며 Ramp input을 통하여 이차원 모델에서의 이동열원의 영향을 고려하였고 실험치와의 비교에서 최적 ramp 시간을 결정하였다. 다층용접에서는 용접 pass에 비례하여 계산시간이 증가한다. 따라서 후판용접의 잔류응력계산에는 막대한 계산시간이 필요하며 이를 줄이기 위하여 Lumped 모델을 개발하였다. 이 Lumped 모델에서는 각 용접층에 들어있는 용접 pass들을 하나의 lumped pass로 이용하였으며 각 pass를 따로 계산한 모델 및 시험치와의 비교를 통하여 최적 lumped technique을 제시하였다.

Abstract

Finite element models were developed for thermal and residual stress analysis for the specific welding problems. They were used to evaluate the effectiveness of the various welding heat input models, such as ramp heat input function and lumped pass models. Through the parametric studies, thermal-

* 정회원, 삼성항공산업(주) 특수CAE팀.
** 정회원, 대우조선공업(주)

mechanical modeling sensitivity to the ramp function and lumping techniques was determined by comparing the predicted results with experimental data. The kinetics for residual stress formation during welding can be developed by iteration of various proposed mechanisms in the parametric study.

A ramp heat input function was develped to gradually apply the heat flux with variable amplitude to the model. This model was used to avoid numerical convergence problems due to an instantaneous increase in temperature near the fusion zone. Additionally, it enables the model to include the effect of a moving arc in a two-dimensional plane. The ramp function takes into account the variation in the out of plane energy flow in a 2-D model as the arc approaches, travels across, and departs from each plane under investigation.

A lumped pass model was developed to reduce the computation cost in the analysis of multipass welds. Several weld passes were assumed as one lumped pass in this model. Recommendations were provided about ramp lumping techniques and the optimum number of weld passes that can be combined into a single thermal input.

1. INTRODUCTION

Fusion welding processes are commonly used to join structural members. These welding processes generally employ a moving heat source that attains a high enough temperature to melt the material at the joint. The resulting temperature distributions are highly nonlinear. Nonuniform expansion on heating and contraction on cooling in weld area give rise to large local stresses which usually lead to plastic deformation. As a result, residual stresses are retained in the weldments after welding.

Analysis of welding heat flow problems includes heat generation by the welding arc, heat loss by convection and radiation, and heat conduction with boundary conditions and initial conditions. A weldment responds to the welding heat source by undergoing physical changes of melting and solidification, solid phase transformation, creation of transient stresses and strains. Investigations of these metallurgical and mechanical responses require thermal modeling and procedural analysis of the arc heat input of the welding process . Modeling heat input from the arc is the most critical task, for it directly influences temperature profile, cooling rates, size of the fusion zone (FZ) and heat affected zone (HAZ), and consequently the microstructure and strength of the weldment.

In this study, several different heat input models were investigated and the sensitivity and efficiency of each model were compared and experimentally verified.

There have been many publications on weld modeling using finite element(FE) methods. The majority of the efforts, however, are focussed on development of elaborate numerical techniques for the study of the weld pool physics rather than for the prediction of residual stresses in realistic structures. In this study, efforts have been made to develop simplified FE procedures so that realistic temperature/stress histories in a weldment can be simulated with commonly available FE analysis package[1)]. Representative works along this line are 2-D model with a ramp heat input function and lumped model.

Since the critical residual stresses and metallurgical zones are formed around the arc during welding, precise thermal conditions such as nonlinear ramp heat input functions are needed to accurately predict the residual stress distribution. However, to date the influence of ramp heat input function on temperature predictions for near weld regions has not been studied. Parametric ramp function studies need to be conducted to develop a FE analysis procedures for predicting various metallurgical zones and resultant residual stress in the weldment.

Lumped pass models were developed for thermal and stress analysis to reduce computation time. A lumped pass model is especially cost effective for simulation of multipass welds. Several different techniques for lumping the ramp functions were investigated and experimentally verified in this study. Modeling sensitivity to weld lumping was determined through parametric studies. Change in joint rigidity and neutral axis in the weld cross-section after completion of each weld pass was studied to determine the kinetics of lumping effect.

The two-dimensional modeling procedure for weldment residual stress predictions was developed based on observations of the thermal-mechanical behavior of weldments during welding. A cross section of weldment with unit width can be modeled with a ramp heat input function to determine both temperature and stress histories in a three-dimensional weldment. In addition, stresses caused by intermediate weld passes laid between root passes and cap passes are cumulative. Multiple weld passes can therefore be appropriately lumped together in the modeling procedure to reduce the computational time. Residual stresses can be numerically determined with a reasonable computational effort.

The base material used in this study was ASTM A36 mild steel. The GMAW process was selected for modeling. The development of a finite element model requires three steps ; thermal model using the ramp heat input function, mechanical model, and lumped pass model. As previously discussed, the 2-D model was used for both the thermal and stress analyses. Identical finite element meshes and time steps were employed. The commercial finite element code, ABAQUS, was used for temperature and residual stress calculations. Eight-node elements were used for the thermal models and ten-node generalized plane strain elements were used for the mechanical models.

2. RAMP HEAT INPUT MODEL

2.1 Heat Input Energy of an Arc Welding

Modeling heat input from the arc is critical task. It directly influences the temperature profile, cooling rate, size of the fusion zone and heat affected zone, and consequently the microstructure and weld metal strength. The loss of energy that occurs from arc to plate is extremely complex in nature and to avoid this complexity a term called arc effeciency is used to quantify the energy made available to the welding plates by the arc. Net heat input from the arc to the weldment is expressed by the following equation :

$$Q=\eta EI \tag{1}$$

where Q is net heat input from the arc(thermal power), η is arc efficiency, E is arc voltage and I is current.

Careful consideration must be exercised in choosing a value of arc efficiency because predicted temperatures are sensitive to change in arc efficiency. Peak temperatures at locations in and around the weld pool change approximately the same as the change in arc efficiency.

Arc efficiency, η, is dependent upon the welding process, metal transfer mode, shielding gas, and other factors, making it very difficult to predict. Christenen et al.[2] and Rykalin[3, 4] extensively measured the arc efficiency of various welding processes using the calorimetry method. In this study, an arc efficiency of 85 percent was adopted for the GMA welding of mild steel.

A two-dimensional FE model using ramp heat input functions and lumped weld passes has been used to predict the thermal and mechanical responses of the weldments. The 2-D modeling of the weld process is illustrated in Fig. 1 and is based on the assumption of a quasi-stationary state.

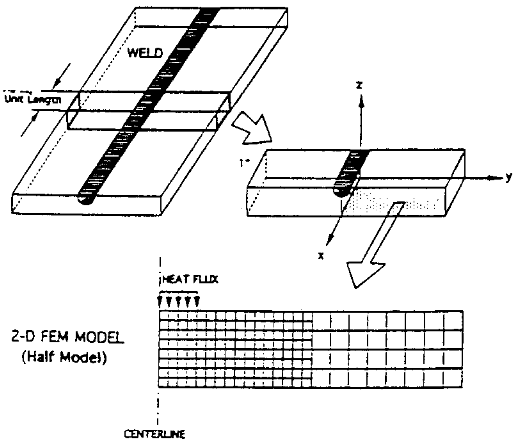

Fig. 1 Two dimensional finite element model of the weldment

2.2 Ramp Heat Input Model

The general amplitude versus time curve for the ramp heat input function is shown in Fig. 2. The actual welding time for the arc to travel across the unit thickness of the model is t_1+t_2. The magnitude of 1/V represents this heat scanning time. The temperature profiles are affected by the ramp time percentage, which is defined to be

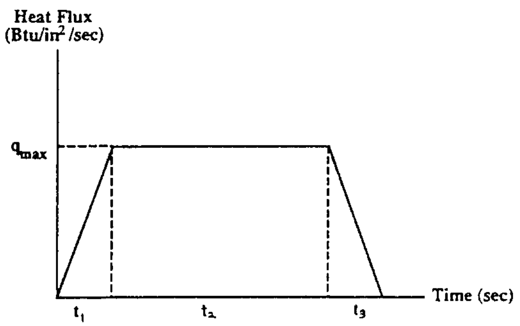

t_1 : Initial Ramp Time
t_2 : Maximum Ramp Time
t_3 : Decaying Ramp Time
t_1+t_2 : Actual Heat Scanning Time during Welding
Ramp Time Percentage$=100t_1/(t_1+t_2)$

Fig. 2 Shape of the ramp heat input function

$$\text{Ramp time percentage} = \frac{t_1}{t_1+t_2} \times 100 \qquad (2)$$

Heat input energy per unit length and heat flux were calculated by the following equations :

$$\text{Heat Input Energy} : H = \frac{\eta EI}{1055} \times \frac{60}{V} \qquad (3)$$

$$\text{Heat flux} \quad -\text{Body flux} : q = \frac{\eta EI}{1055V_e} \qquad (4)$$

$$-\text{Surface flux} : q = \frac{\eta EI}{1055bL} \qquad (5)$$

where H = heat input energy per unit length, Btu/inch
η = arc efficiency
E = arc voltage, volts
I = arc current, amps
V = welding speed, inches per minute
60 = conversion factor, minute to seconds
1055 = conversion factor, Joule to Btu
q = heat flux, Btu/in^2-sec(for surface heat flux) Btu/in^3-sec(for body heat flux)
V_e = volume of bead elements in which heat flux is in, in^3
b = total width of deposited bead elements, inch
L = length of heat input area in welding direction(unit length in two-dimensional model), inch.

The heat transfer and stress analysis of thick plate weldments require a large amount of computing time. Therefore, a very simple model was utilized for the parametric study of heat input modeling techniques. Single pass bead-on-plate GMA welds on 1/2 inch thick plate was used for the ramp effect study.

Fig. 3 shows the weld bead configuration, welding parameters, and heat input data used for the finite element model. As shown in Fig. 3(b), surface heat flux covers the weld bead area at the top surface of the plate. The magnitude of net heat input energy and heat flux was calculated using Equations 4 and 5.

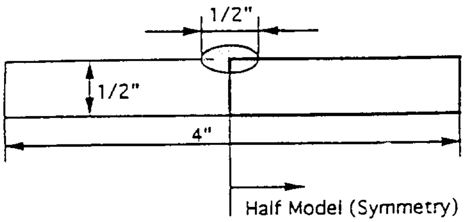

(a) Model dimensions and bead configuration

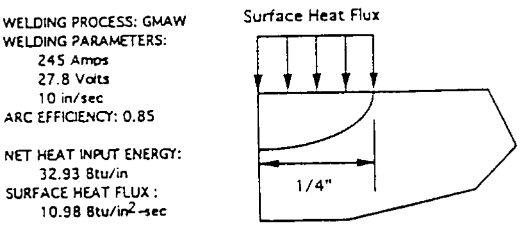

(b) Welding parameters and heat input data

Fig. 3 Single pass bead-on-plate weld on the 1/2″ thick plate

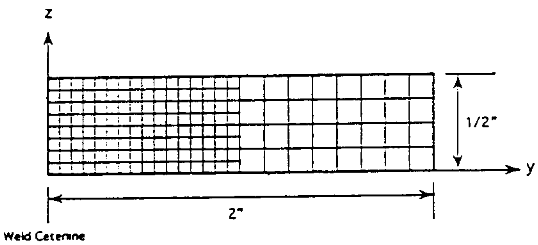

(a) Finite element mesh and model dimensions

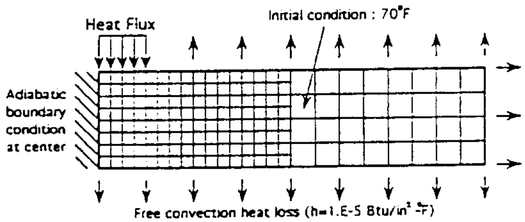

(b) Thermal model with boundary conditions

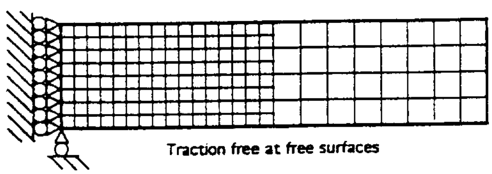

(c) Mechanical model with boundary conditions

Fig. 4 2-D finite element models and boundary conditions(single pass bead-on-plate weld on the 1/2″ thick plate)

Fig. 4 shows the 2-D finite element mesh and boundary conditions in thermal and mechanical models. Only half the plate was modeled with symmetry boundary conditions at the weld centerline. ABAQUS eight-node rectangular elements were used for the thermal ananysis and ten-node generalized plane strain elements were adopted for the stress analysis. Both models use 160 elements and 545 nodes and identical mesh layouts.

2.3 Effect of Ramp Time on Thermal and Mechanical Analysis

Various ramp times from 0 to 100 percent of the actual welding time over a unit weld length were used to monitor the sensitivity of the ramp heat input model. Fig. 5 shows the ramp functions with different ramp time percentages for a weld speed of 10 inches per minute. The same magnitude of the heat flux, 10.98 Btu/in^2-sec, and actual welding time(t_1+t_2 in Fig. 2), 6 seconds, were used in all cases. The area under the ramp function curve was kept constant to maintain the same net heat input energy and study the effect on thermal and stress responses.

(a) Ramp time=0%　　(b) Ramp time=20%

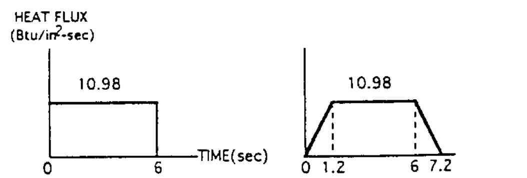

(c) Ramp time=50%　　(d) Ramp time=100%

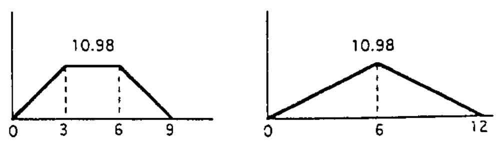

Fig. 5 Ramp functions for different ramp times

Fig. 6 shows the temperature profiles at points which are 1/4 inch and 1/2 inch from the weld centerline on the top surface. The trend shows that large ramp times causes a decrease in peak temperature and cooling rate in the near weld region. Moving away from the weld, the effects tend to be less at the peak temperature. The temperature profiles of large ramp times were shifted to the right, which indicates that more time was required to reach peak temperature. The time to reach the peak temperature is related to the total heat scanning time($t_1+t_2+t_3$ in Fig. 2).

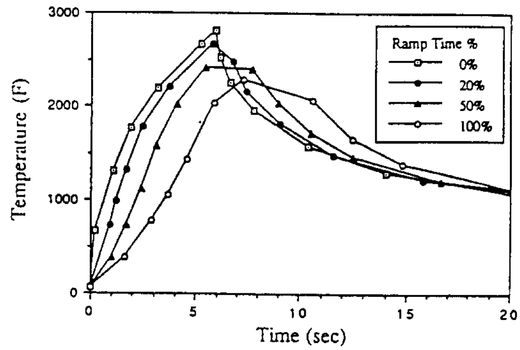

(a) Temperature profiles at 1/4″ from the weld center (top surface of the plate)

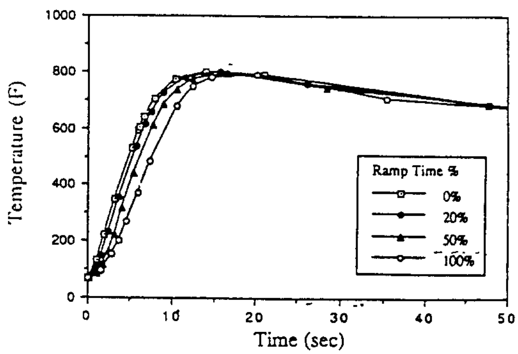

(b) Temperature profiles at 1/2″ from the weld center (top surface of the plate)

Fig. 6 Temperature profiles at 1/4 inch and 1/2 inch from the centerline(single pass bead-on-plate welding of the 1/2 inch thick plate)

Fig. 7 shows the distribution of longitudinal and transverse residual stresses on the top surface. It was observed that in contrast to the thermal results, ramp time does not significantly affect the residual stresses for a given welding condition. Maximum values of longitudinal stress and transverse stress are constant, regradless of the ramp time percentages. The tensile stress zone for small ramp time was slightly larger, but it is negligible.

The concept of a sensitivity area was adopted to describe this phenomenon. As shown in Fig. 6, different ramp times result in peak temperature variations only at the near weld region which has the highest temperatures. The formation of residual stress is strongly dependent upon the mechanical properties of the specimen.

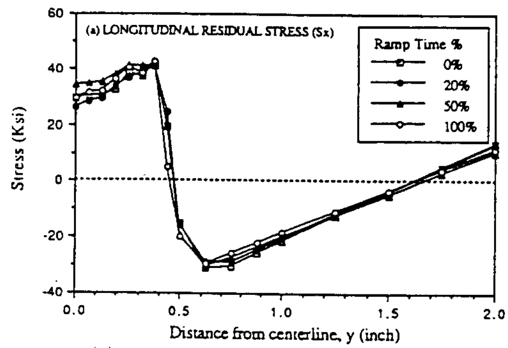

(a) Longitudinal residual stress(Sx)

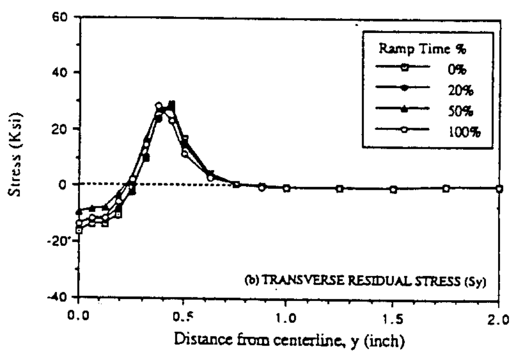

(b) Transverse residual stress(Sy)

Fig. 7 Residual stress at the top surface of the plate for different ramp times

Fig. 8 shows temperature-dependent mechanical and physical properties of ASTM A36 steel. Both the elastic modulus and yield stress decrease with increasing temperature. There is a division point in these values versus temperature curve. Above this point they decrease at an accelerated rate with increasing temperature. As shown in Figure 8, mild steel looses strength at an accelerated rate above 1000°F and therefore contribution to residual stress due to temperatures above 1000°F is expected to be small.

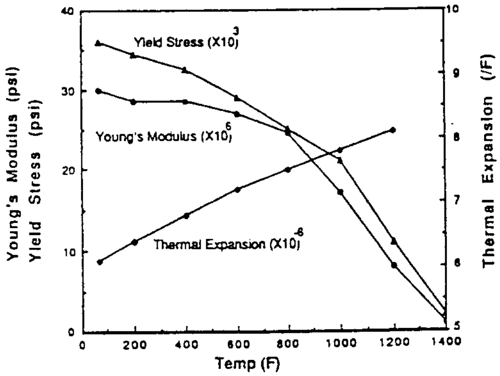

Fig. 8 Temperature-dependent mechanical properties of ASTM A36 steel

As described above, the high temperature region is not a major contributor to the residual stress due to lower yield stress and elastic modulus at elevated temperatures. Therefore, the final stress is not sensitive to ramp times as shown in Figure 7. The isotherm plots of 20% and 50% ramp time in the transverse cross section(y-z plane) are in Fig. 9(a) and 9(b) with different time steps. The isotherms at near arc regions in the top surface of the plate(x-y plane) are in Fig. 9(c). These clearly show that low temperature regions under 1000°F, which are dominant in determining residual stress are insensitive to ramp time.

These results show that the model with smaller

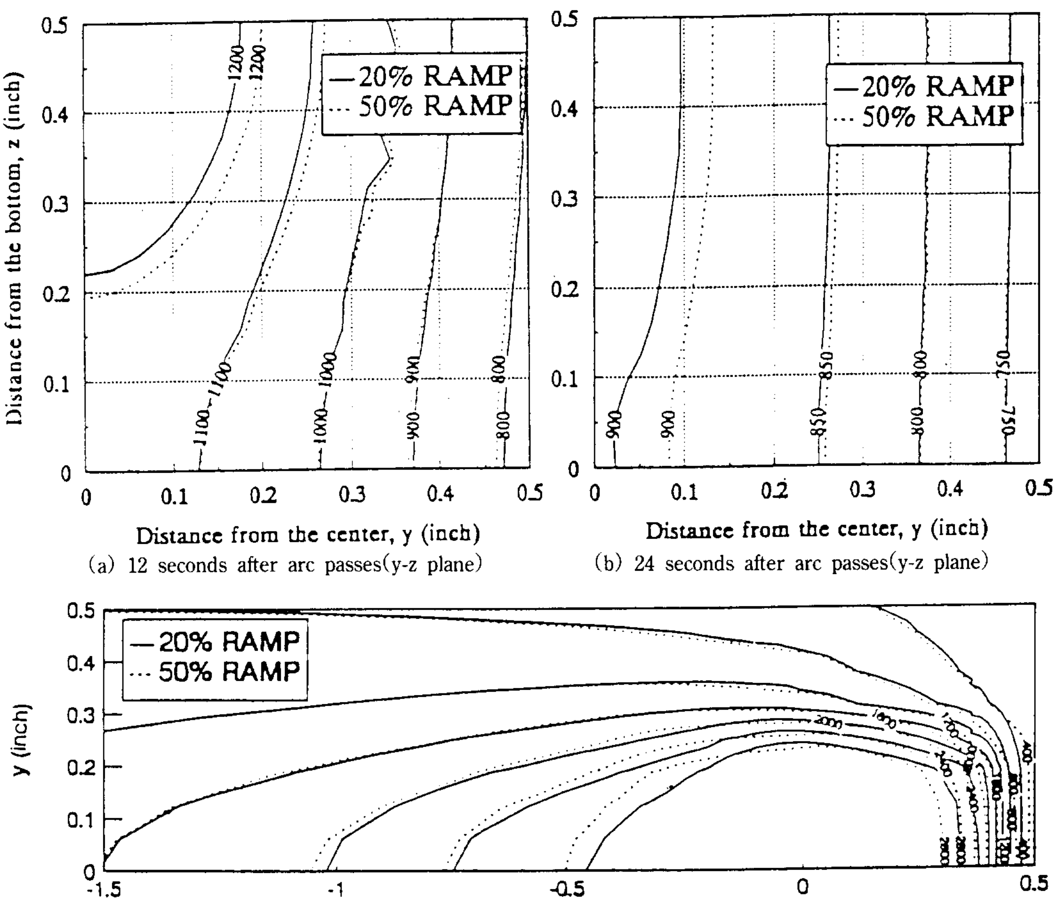

(a) 12 seconds after arc passes(y-z plane)

(b) 24 seconds after arc passes(y-z plane)

(c) temperature fields at near arc region(x-y plane)

Fig. 9 Temperature fileds for ramp times of 20% and 50%

ramp time required slightly more computational time and numerical cycles than other models with larger ramp time. It is primarily due to the faster thermal response and sharper temperature gradient that exists in the small ramp time model near the weld. From a comparison with the experimental results[5](Fig. 10), it was determined that a ramp time of 20% provides the most accurate results in thermal analysis. Therefore, the ramp time of 20% is used for subsequent thermal analyses.

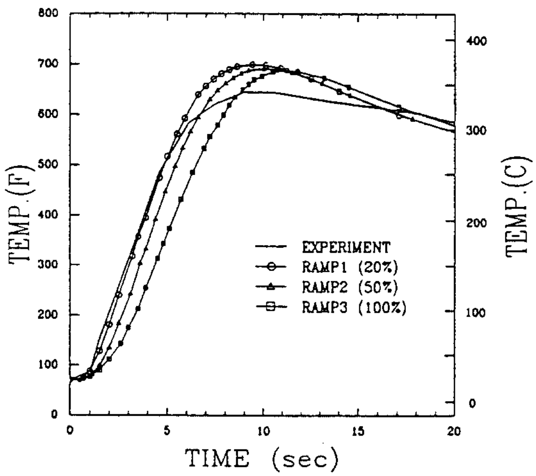

Fig. 10 Temperature profiles of various ramp time percentages for the first pass on 1/2-inch thick plate, located 1/4 inch from the weld centerline at the top surface.

2.4 Effect of Heat Input Mode

Different types of heat flux and distribution pattern can also be utilized for finite element analysis. In this study, the following heat input modes were investigated :

1. Uniformly distributed heat flux over a given area (surface flux)
2. Gaussian distribution of surface flux
3. Uniformly distributed heat flux over a given volume(body flux)

The optimum heat input modeling schemes were drawn from the results of these parametric analyses. Finite element models are same as previous models used for ramp study.

The temperature field is significantly affected by the heat flux type and its distribution pattern in the regions near the weld. Fig. 11 compares the size of the FZ and HAZ determined by heat flux models and experiments. Isotherms of melting point(2800°F) and the A3 phase transformation temperature(1600°F) of mild steel represent the location of the FZ and HAZ. Surface flux(uniform or Gaussian distribution) and body flux (uniform distribution) were each considered.

From a comparison with the experimental results (see Figure 11), it was noted that when the surface or body flux was uniformly distributed over the top layer of the weld bead elements, the model produced a more accurate temperature field at the near weld regions than Gaussian distribution of surface flux. The model produced a wide and shallow FZ and HAZ, which are very similar to the actual bead configuration produced by a bead-on-plate GMA welding. Another advantage of uniformly distributed surface flux model is the convenience in heat input modeling. Often the exact shape of the weld bead(penetration depth) may not be known during the numerical analysis. Heat distribution over the top layer of the weld bead elements is considered a more practical approach.

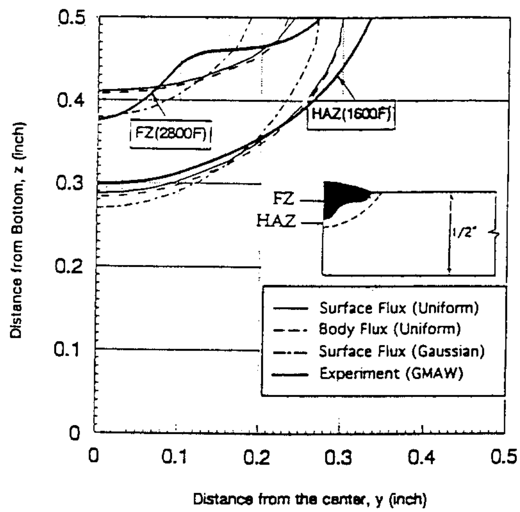

Fig. 11 Size of FZ and HAZ determined by different heat flux models(single pass bead-on-plate welding of the 1/2 inch thick plate)

The formation of the fusion zone involves many mechanisms such as arc force, fluid dynamics, convection and radiation heat losses. These items are not considered in this model. However, simple heat conduction model developed in this study with an appropriate heat input scheme could simulate the FZ in an acceptable accuracy as shown in Fig. 11.

The surface flux required almost the same computation time and numerical cycles as the body flux, and much less time than the concentrated heat flux without any loss in accuracy. Therefore, the use of surface flux or body flux is acceptable for thermal analysis of weldments.

3. LUMPING TECHNIQUES FOR MULTI-PASS WELDS

In the previous work[5, 6], it was observed that after mechanical constrains are built up by initial weld passes, subsequent passes affect residual stress distribution in a local area only. Based on this phenomena, a method of grouping weld passes was used to reduce the computing cost. In the lumped pass models, the individual beads in a layer were combined, and the combined total heat flux of the individual beads was distributed over the weld bead elements of the whole layer.

Very few investigators have studied lumped pass modeling techniques. Rybicki and Stonisifer[7] studied multipass girth pipe welds by combining all passes in a layer into a single stress analysis sequence. In a thirty pass, nine layer weld up to a maximum of four passes per layer were combined. Their results partially agreed with the experimental data. They only used these lumping techniques for the stress analysis, therefore, no saving of computation time was realized in the heat transfer analysis and all weld passes must be simulted. After the temperature distributions for each pass were obtained, the maximum temperatures experienced at the grouped elements were determined. These temperatures, which are an envelope of the temperature distributions of all passes, were submitted to the stress analysis model as though they were obtained from the temperature distribution of a single layer of passes. This approach requires additional time for temperature data processing and, thus, is difficult to handle in multipass welding analysis.

Leung and Pick[8] proposed the same approach as Rybicki's work. They studied several simplification techniques including lumping method in a three pass weld. Their work was limited to the analysis of small number of weld passes. Ueda *et al.*[9] also investigated the lumping technique. They grouped two weld passes, therefore, like Leung's work, their results could not provide the complete picture of the effect of lumping techniques which usually group more passes in multipass welds.

A different approach was proposed, in this study, to improve the efficiency of a lumped pass model. The following section presents the results of the multipass weld analysis, using refined lumping techniques.

3.1 Ramp Lumping Techniques

The ramp functions shown in Fig. 12(a) represent three individual passes for a non-lumped model. From an early study on the modeling varialbes, it was noticed that two factors, maximum flux magnitude and heat scanning time, dominantly affect the predicted residual stress distribution [6]. To include the total heat input energy of each actual weld pass, the area under a combined ramp function used for a lumped model should equal the sum of the areas under the individual ramp functions which represent the actual weld passes. This may be accomplished by selecting appropriate values for maximum flux magnitude and heat scanning time.

Two alternative ramp models used for the lumped pass models in this study are presented schematically in Fig. 12(b) and 12(c). The first model is referred to as a "RAMP 1" technique. In this model, the heat scanning times for each pass were summed and the magnitudes of heat flux of the individual passes were averaged. In the second ramp model, inversely to the first model, heat flux magnitudes were accumulated and heat scanning times were averaged, as shown in Fig. 12(c). This model is referred to as a "RAMP

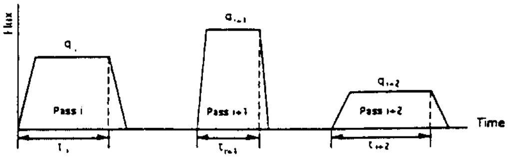

(a) Ramp functions of welding passes before lumping

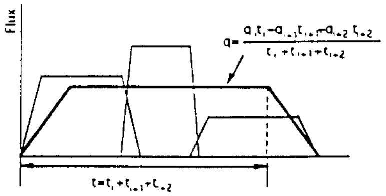

(b) Ramp function after lumping(RAMP 1)

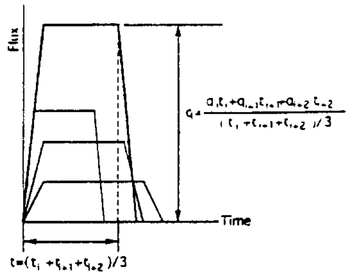

(c) Ramp function after lumping(RAMP 2)

Fig. 12 Ramp functions of heat input before and after lumping

2" technique.

Both ramp models were analyzed to evaluate their effectiveness for 1 inch and 2 inch thick plate with double-V groove. Pass sequences, welding parameters, and finite element meshes for 1 inch and 2 inch thick plates were shown in Fig. 13 and 14, respectively. 11 weld passes were reduced to 6 lumped passes for 1 inch thick plate, and 38 weld passes were reduced to 14 lumped passes for 2 inch thick plate. The results from lumped model were compared to the non-lumped model and experiment in Fig. 15 and 16[10].

These figures show residual stress distributions at the top surface of the 1-inch and 2-inch thick plates. RAMP 1 model shows a better correlation with the non-lumped model and the experiment than RAMP 2 model. The stress distribution of the RAMP 1 model almost coincides with the non-lumped model results and experimental data as shown on Fig. 16.

RAMP 2 model generally produces a larger tensile stress zone than other models and shows considerable change in the magnitude of maximum tensile and compressive stresses. Ramp function of RAMP 2 model represents a welding process which has higher arc power and faster welding speed. This heat input pattern increases the temperature gradient and, conse-

Pass Sequence	Pass No.	Welding Parameters		
		Current (A)	Voltage (V)	Speed (IPM)
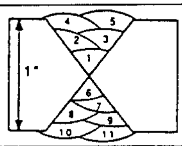	1	190	25	7.9
	2−5	215	26	11.1
	6	190	25	7.9
	7−9	220	26	11.1
	10−11	250	27	11.1

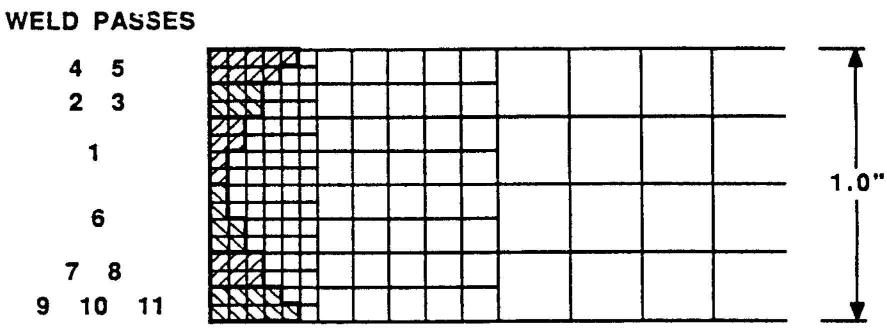

Fig. 13 Pass sequence, welding parameter, and finite element mesh for 1 inch thick plate with double-V groove

Pass Sequence	Pass No.	Welding Parameters		
		Current (A)	Voltage (V)	Speed (IPM)
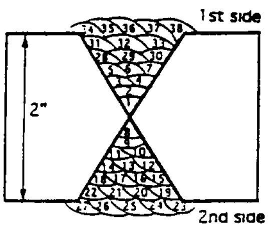	1−4	250	26.5	8.0
	5−7	250	26.5	13.0
	8−9	230	26.5	10.0
	10−14	240	26.5	13.0
	15−18	230	26.5	14.5
	19−22	220	27.0	13.0
	23−27	230	26.5	12.0
	28−30	230	26.5	12.0
	31−38	240	26.5	13.0

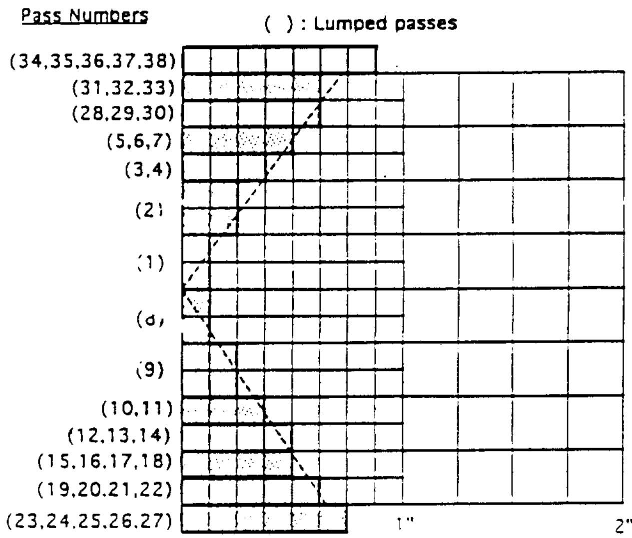

Fig. 14 Pass sequence, welding parameter, and finite element mesh for 2 inch thick plate with double-V groove

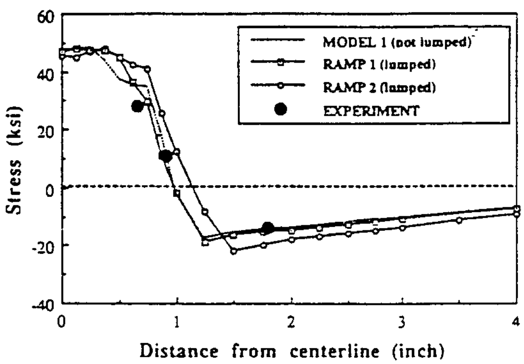

Fig. 15 Longitudinal residual stress distribution at the top surface of the 1-inch thick plate with double-V groove

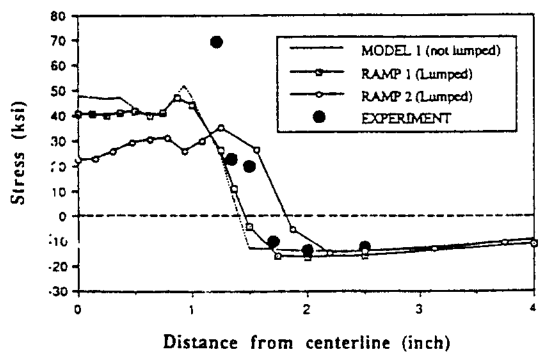

Fig. 16 Longitudinal residual stress distribution at the top surface of the 2-inch thick plate with double-V groove

quentially, results in a change of the residual stress distribution. However, from a comparison with the experimental data and the non-lumped model results, it is noted that RAMP 2 model over-estimates the heat input rate. Another deficiency of RAMP 2 model is the computation time. This model required about 20% more CPU time and increments than the RAMP 1 model, due to the large temperature gradient existing at the weld area. From these results, the RAMP 1 model is considered accurate and most efficient.

3.2 Limitations of Lumped Pass Model

Lumped pass models combine the thermal and mechanical responses of each weld pass and produce an envelop of those individual weld pass results. In the models for 1-inch and 2-inch thick plate with double-V groove, very good correlations were obtained between the lumped models and the measured data.

Fig. 17 shows the analysis results of a 1-inch thick plate with single-V groove[10]. 17 weld passes were reduced to 7 lumped passes in the lumped model. Unlike previous models, the lumped pass results show considerable deviations from the non-lumped model results and experimental data. Fig. 18 shows the longitudinal residual strain variations at the weld centerline through the thickness. Longitudinal strains should be linear through thickness in generalized plain strain assumption, but the figure shows non-linear distribution because of different strain histories of each weld bead, for example, second bead starts with zero strain with deformed geometry. While no significant changes were observed in a plate with double-V groove, there are large differences in the strain distributions between the lumped and non-lumped models for a plate with single-V groove. These phenomena occur when the bead depositions are not symmetric about the neutral axis of a weldment. In single-V groove, the center of the total shrinkage force does not coincide with the neutral axis. This results in larger bending stress and produces different final stress and strain states. The lumped pass amplifies this effect. Therefore, small size lumping or individual pass analysis is recommended for a weld which has unsymmetrical bead depositions like a single-V groove weld.

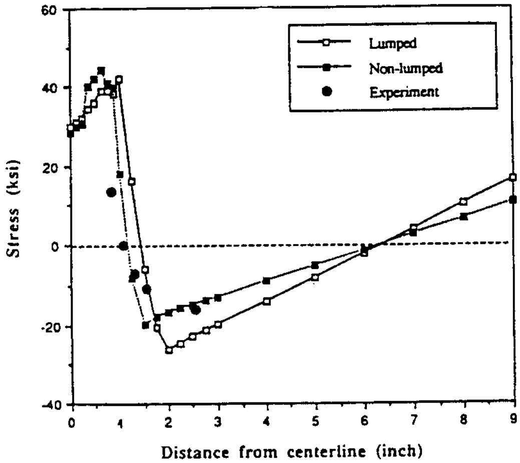

Fig. 17 Longitudinal residual stress distribution at the top surface of the 1-inch thick plate with single-V groove

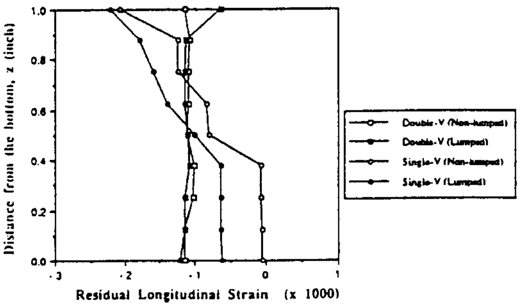

Fig. 18 Longitudinal residual strain variations at the weld centerline through the thickness

4. CONCLUSIONS

The two-dimensional modeling procedure for weldment residual stress predictions was developed based on observations in the thermal-mechanical behaviors of weldments during welding. Welding stresses are primarily governed by the quasi-steady thermo-mechanical state. A cross section of weldments with unit width can be modeled with a ramp heat input function to determine both temperature and stress histories in a three-dimensional weldment. The insensitivity of mechanical response to high temperature material volumes in the weldment makes the ramp function effect relatively insignificant. In additions, stress caused by intermediate weld passes laid between root passes and cap passes are cumulative. Multiple weld passes can therefore be appropriately lumped together in the modeling procedure to reduce the computational time. Residual stresses can be numerically determined with a reasonable computational effort.

The parametric study using a simple model for a single or multiple pass bead-on-plate weld is a valuable tool which may be used to produce basic information for developing or refining finite element models with minimized cost and time. From the parametric study on the heat input mode, it was observed that the thermal responses at the near weld regions are significantly influenced by the following inputs : ramp time, heat source size, heat flux type, and distribution pattern. Therefore, these terms should be carefully selected to accurately predict temperature profiles, cooling rates, size of FZ and HAZ, and the resultant microstructure. The following scheme is recommended for thermal analysis :

-20 percent ramp time and process dependent ramp function

-heat input over the actual bead size

-body flux or surface flux uniformly distributed over the top layer of the weld bead elements

The recommended heat input parameters do not influence the temperature fields at regions far away from the weld. Consequently, the residual stresses which are determined by low temperature regions are insensitive to those parameters. This characteristic of insensitivity to the heat input mode provides an avenue for further simplification in the stress model. This is the lumped pass model.

The accuracy of the lumped pass model is dependent upon the lumping method. A "stepped over" lumping technique which uses an averaged heat flux magnitude and an accumulated heat scanning time for the number of passes lumped was introduced in this study. Lumped pass models which include this technique produce accurate results in an efficient manner. The lumping of one layer of weld beads is considered optimum. The residual stress distribution is affected primarily by the first few passes and subsequently by the final capping passes. Intermediate passes do not significantly affect the residual stresses. Therefore, no lumping or lumping a small number of passes is recommended for the first few passes and final capping passes. For the intermediate passes, a large number of passes may be lumped.

The lumping of the final capping passes results in a large deviation from the non-lumped model results for a weld which has unsymmetrical bead depositions like a single-V groove weld. Therefore, small size lumping or individual pass analysis is recommended for this weld.

LIST OF REFERENCES

1. ABAQUS User's Manual, HKS Company, 1984
2. Christensen, N., Davies, V. de L., and Gjermundsen, "Distribution of Temperatures in Arc Welding", British Welding Journal, Vol.12, No.2, 1965, pp. 54~75
3. Rykalin, N.N. and Nikolaev, A.V., "Welding Arc Heat Flow", Welding in the World, 9(3/4), 1971, pp.112~132
4. Rykalin, N.N., "Energy Sources Used for Welding", Welding in the World, 12(9/10), 1974, pp.227~247
5. "Determination of Residual Stress and Effects in Thick Section Weldments for Hydraulic Structures", Project Report, Department of Welding Engineering, The Ohio State University, 1990
6. Shim, Y., Feng, Z., Lee, S., Kim, D., Jaeger, J., and Tsai, C.L., "Modeling of Welding Residual Stresses", Proceedings of the Winter Annual Meeting of the ASME, Atlanta, Georgia, Dec. 1991, pp.29~41
7. Rybicki, E.F. and Stonesifer, R.B., "Computation of Residual Stresses due to Multipass Welds in Piping Systems", Journal of Pressure Vessels Technology, Trans. of ASME, 101, May, 1979, pp. 149~154
8. Leung, C.K. and Pick, R.J., "Finite Element Analy-

sis of Multipass Welds", WRC Bulletin 356, Aug. 1990, pp.11~33

9. Ueda, Y., Takahashi, E., Fukuda, K., and Nakacho, K., "Transient and Residual Stresses in Multi-Pass Welds", Transactions of JWRI, 3(1), 1974, pp.59~67

10. "Experimental Verification of Finite Element Modeling Procedures for Thick Plates", Technical Report submitted to U.S. Army Corps of Engineers, Department of Welding Engineering, The Ohio State University, 1992